Crystallographic Study of Yeast Copper Amine Oxidase

RONGBAO LI,[a] LONGYIN CHEN,[a]† DANYING CAI,[b]† JUDITH P. KLINMAN[b] AND F. SCOTT MATHEWS[a]*

[a]*Department of Biochemistry and Molecular Biophysics, Washington University School of Medicine, St Louis, MO 63110, USA, and* [b]*Department of Chemistry, University of California, Berkeley, CA 94720, USA. E-mail: mathews@fsmiris.wustl.edu*

Abstract

The copper-containing amine oxidase from the yeast *Hansenula polymorpha* (YAO) has been crystallized and partially solved by molecular replacement. It catalyzes the oxidative deamination of primary amines by molecular oxygen to the corresponding aldehydes, ammonia and hydrogen peroxide. It contains a covalently bound redox cofactor, topa quinone, generated by post-translational modification of a single tyrosine side chain. The crystals of YAO are orthorhombic, with space-group symmetry $P2_12_12_1$ and unit-cell dimensions $a = 138.8$, $b = 148.2$, $c = 234.0$ Å and diffract X-rays beyond 2.0 Å resolution. Solution by molecular replacement using the *E. coli* amine oxidase structure [Parsons, Convery, Wilmot, Yadav, Blakeley, Corner, Philips, McPherson & Knowles (1995). *Structure*, **3**, 1171–1184] as a search model reveals that there are three dimers in the asymmetric unit in a trigonal arrangement having 32 point-group symmetry. The solution agrees well with the self-rotation function of YAO. The non-crystallographic threefold axis lies parallel to a crystallographic twofold screw axis and each dimer has twofold symmetry. Phases from the refined model based on the molecular-replacement solution were used to solve one heavy-atom derivative. Model building from the unbiased isomorphous replacement phases is in progress.

1. Introduction

Copper-containing amine oxidases (CAO, E.C. 1.4.3.6) form a class of enzymes which is widespread in nature and has been studied from a variety of organisms including bacteria, yeast, plants and mammals (McIntire & Hartmann, 1992; Klinman & Mu, 1994; Knowles & Dooley, 1994). CAO's catalyze the oxidation of primary amines by molecular oxygen to the corresponding aldehydes, ammonia and hydrogen peroxide. The substrates of the enzymes, including monoamines, diamines and polyamines are involved in various biological processes (Bachrach, 1985; Janne,

Posa & Raina, 1978; McCann, Pegg & Sjoerdsman, 1987) and their levels are regulated by synthesis, degradation and excretion. While ornithine decarboxylase and S-adenosyl-L-methionine decarboxylase provide for biosynthesis of these amines, their catabolism is catalyzed by CAO's which convert them to various compounds of biological importance. CAO's have been implicated in detoxification of biogenic amines, cell growth and differentiation, wound healing and signal processes; consequently, they have become important target enzymes for pharmacological and clinical research. In general, CAO's are homodimeric enzymes with molecular weights in the range of 75–100 kDa. Most of the eukaryotic CAO's are glycoproteins. As metalloproteins, CAO's belong to the biologically important class of type-2 or non-blue copper proteins (Dooley *et al.*, 1991).

In early studies, CAO's were shown to be quinoproteins, containing a reactive carbonyl group which led to a hypothesis that pyridoxal phosphate was a cofactor (Hamilton, 1968); later, the cofactor was proposed to be a covalently bound pyrroloquinoline quinone (PQQ) (Lobenstein-Verbeek, Jongejan, Frank & Durine, 1984; Ameyama, Hayashi, Matsushita, Shinagawa & Adachi, 1984). In 1990 it was demonstrated by mass spectroscopy and NMR studies that PQQ is not the cofactor of CAO (Janes *et al.*, 1990; Mu, Janes, Smith, Brown, Dooley & Klinman, 1992). Instead the cofactor was shown to be the modified side chain of a gene-encoded tyrosine residue on the protein polypeptide chain, 2,4,5-trihydroxyphenylalanine, or topa quinone (TPQ). This has been recently verified by crystal structures of copper amine oxidases from *E. coli* and from pea seedling (Parsons *et al.*, 1995; Kumar *et al.*, 1996).

The existence of topa quinone has been demonstrated in CAO's from a variety of different sources (Janes & Klinman, 1995). The precursor tyrosine residue (Tyr‡) has been located in a highly conserved consensus sequence, Thr-*X*-*X*-Asn-Tyr‡-Asp/Glu (Janes *et al.*, 1992). TPQ formation appears to occur *via* a self-catalytic mechanism in which a tyrosine residue is oxidized by protein-bound copper and oxygen (Cai & Kinman, 1994*a*; Matsuzaki, Fukui, Sato, Ozaki & Tanizawa, 1994; Fontecave & Eklund, 1995). The proposed catalytic mechanism for amine oxidation

---

consists of two half-reactions (Klinman & Mu, 1994; Hartmann & Dooley, 1995): a reductive half-reaction and an oxidative half-reaction. In the reductive half-reaction, the amine is oxidized to the aldehyde and the enzyme becomes reduced through formation of a Schiff-base complex. The oxidative half-reaction leads to reoxidation of the enzyme by oxygen and release of ammonium ion. The copper is required for this step of the reaction, in addition to its role in TPQ biosynthesis. During the oxidative half-reaction an aminosemi-quinone radical intermediate is generated.

Yeast amine oxidase (YAO) is localized in the peroxisomes of the methylotrophic yeast *Hansenula polymorpha* (Zwart, Veenhuis, van Dijken & Harder, 1980; McIntire & Hartman, 1992). At least two isoforms are present, one with preference for aromatic amines (benzylamine oxidase) and the other for small aliphatic amines (methylamine oxidase). The methyl-amine oxidase isoform of YAO has been overexpressed in *Sacchromyces cerevisiae* (Cai & Klinman, 1994b). It has a subunit molecular weight of 78 kDa and is about 2% glycosylated. Its amino-acid sequence is approximately 35% identical to *Arthrobacter* CAO, 28% identical to *E. coli* amine oxidase and about 23% identical to other eukaryotic CAO's (Tipping & McPherson, 1995). YAO has been studied extensively, and considerable spectroscopic and mechanistic data exist for the wild-type enzyme and for a number of site-
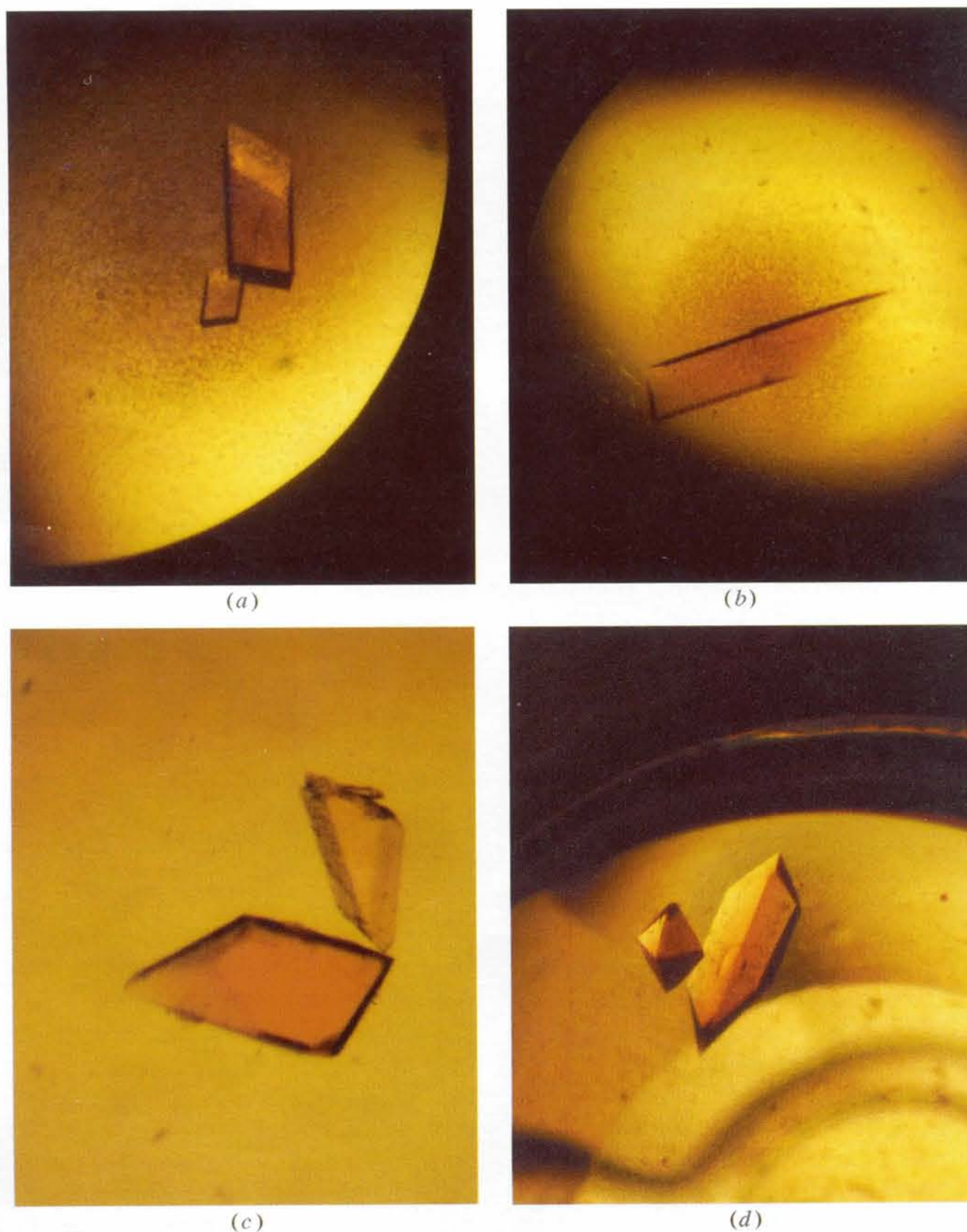

Fig. 1. Crystals of yeast copper amine oxidase. There are four polymorphs observed under the same crystallization conditions: (a) and (b) are monoclinic crystals and (c) and (d) are orthorhombic crystals.

specific mutants (McIntire & Hartmann, 1992; Klinman & Mu, 1994). Full interpretation of these data awaits a molecular structure. As a first step, we report here a preliminary crystallographic study of recombinant copper amine oxidase from the yeast *H. polymorpha* expressed in *S. cerevisiae*.

2. Materials and methods

2.1. Enzyme preparation

The YAO gene from the methylotrophic yeast *H. polymorpha* was expressed in *S. cerevisiae* with the yeast expression vector *p*BD20 controlled by the alcohol dehydrogenase (ADHI) promoter. The plasmid construction and purification procedures for the recombinant YAO were reported elsewhere (Cai & Klinman, 1994*b*) and have been modified here to obtain a large-scale protein preparation suitable for crystallization. Harvested cells, grown from 12 l of cell culture at 303 K, were resuspended in 0.1 *M* potassium phosphate buffer, pH 7.2, incubated with zymolyase and disintegrated by sonication at 273 K. The crude extract was fractionated by a 10–45% saturated ammonium sulfate cut, dialyzed, and further purified by ion-exchange chromatography on DEAE CL-6B followed by gel filtration on Sephacryl S-300 HR. The enzyme-activity assay and protein assay indicated that the purified enzyme had a specific activity of 0.13 unit mg^{-1}. The enzyme was >90% pure as judged on sodium dodecyl sulfate polyacrylamide gel electrophoresis.

2.2. Crystallization and data collection

Crystals of YAO were grown at room temperature by the sitting-drop vapor-diffusion method. The initial crystallization conditions were obtained using the sparse-matrix Crystallization Screen Kit I & II from Hampton (Carter & Carter, 1979; Jancarik & Kim; 1991; Cudney, Patel, Weisgraber, Newhouse & McPherson, 1994); the conditions were then fine tuned by optimizing the concentration of the precipitant and salt and by varying the pH of the buffer. The best conditions for crystal growth were in sitting drops formed by mixing 5 μl YAO (20 mg ml^{-1} in 10 m*M* potassium phosphate buffer, pH 6.5) and 5 μl crystallization solution (7–9% PEG 8K, 0.3 *M* potassium phosphate buffer, pH 6.2) and equilibrating against 0.5 ml of the latter solution for about 4 weeks at room temperature.

X-ray diffraction data from YAO crystals were collected on an R-AXIS IV imaging-plate system mounted on a Rigaku RU-200 rotating-anode X-ray generator. A beam of X-rays (Cu *K*α, λ = 1.5418 Å) was focused and partially monochromated by an Ni filter and a double-mirror focusing system manufactured by Molecular Structure Corporation (MSC). An oscillation range of 1.5° per frame was used with an

Table 1. *Polymorphic crystal forms of YAO*

Crystal form	Space group	Cell dimensions					
		a (Å)	*b* (Å)	*c* (Å)	α (°)	β (°)	γ (°)
Monoclinic							
Form *A*	*C*2	139.6	158.3	234.8	90.0	90.5	90.0
Form *B*	*P*2$_1$	104.0	105.0	235.0	90.0	97.0	90.0
Orthorhombic							
Form *A*	*P*2$_1$2$_1$2$_1$	138.7	145.0	234.0	90.0	90.0	90.0
Form *B*	*P*2$_1$2$_1$2$_1$	138.8	148.2	234.0	90.0	90.0	90.0

exposure time of 15 to 20 min°$^{-1}$. Data collection from crystals of a typical size of 0.4 × 0.2 × 0.2 mm was carried out at 103 K, using a cold gas stream generated by an X-Stream Cooler from MSC; 25% glycerol was added to the crystal bathing medium as cryoprotectant. A helium beam path was used to reduce intensity losses. The data were processed using *DENZO* (Otwinowski, 1993) and merged and scaled using programs in the *CCP*4 package (Collaborative Computational Project, Number 4, 1994).

2.3. Structural analysis

Self-rotation functions were calculated in spherical polar angles using the *CCP*4 program *POLARRFN* (Collaborative Computational Project, Number 4, 1994). Cross-rotation function and translation-function searches and rigid-body refinement were carried out using *AMoRe* (Navaza, 1994). *X-PLOR* (Brünger, 1992) and the molecular graphic display program *O* (Jones, 1978) were used for crystal packing and geometric analysis. *X-PLOR* was also used for model refinement. The crystal density was measured using a xylene-bromobenzene density-gradient column (Low & Richards, 1952). The molecular weight of protein per asymmetric unit (M_p) was calculated using the method described by Matthews (Matthews, 1974). Several heavy-atom compounds were screened to obtain isomorphous derivatives of YAO using the soaking method (Blundell & Johnson, 1976). The scaling of the derivative data against the native was performed using *SCALEIT* in *CCP*4.

3. Results and discussion

3.1. Crystal characterization

Crystals of YAO are pale pink in color and exhibit several different shapes (Fig. 1). Four different polymorphs of YAO crystals were obtained under similar conditions and were characterized by X-ray diffraction (Table 1). Two of them are monoclinic and belong to space groups *C*2 and *P*2$_1$; both forms exhibit high mosaicity and twinning and the crystals appear to consist of multiple layers. The other two forms are orthorhombic and differ slightly in the length of the *b* axis. Orthorhombic crystal form *B* is much more prevalent. Only one data set, a native, was collected from orthorhombic form *A*. For both orthorhombic

Table 2. *Crystal characterization of YAO on R-AXIS IV image plate*

	Native YAO	Derivative (K$_2$HgI$_4$) (5 mM, 5 d)
R_{merge}*	0.052	0.081
Resolution (Å)	2.4	2.6
Redundancy	3.0	4.5
Space group	$P2_12_12_1$	$P2_12_12_1$
Cell edges a, b, c (Å)	138.8, 148.2, 234.0	139.4, 148.1, 233.8
R_{iso}†	—	0.172
Crystal density (g cm^{-3})	1.224	—
Z	12 dimers	12 dimers
V_M (Å^3 Da^{-1})	2.6	—
Solvent content (%)	46.8	—

* $R_{merge} = \sum_h |I(h) - \langle I(h) \rangle| / \sum_h |I(h)|$, $I(h)$ is the measured intensity of reflection h. † $R_{iso} = \sum_h |F(h)_{deriv} - F(h)_{native}| / \sum_h |F(h)_{native}|$, $F(h)$, is the structure-factor amplitude of reflection h.

forms, systematic absences of the $h00$, $0k0$ and $00l$ reflections for odd indices indicate that they belong to the space group $P2_12_12_1$.

At room temperature, YAO crystals are rather radiation sensitive, showing a three- to fourfold drop in intensity during a data collection run. At cryogenic temperature (123–93 K), the crystals are very stable and diffract beyond 2.0 Å resolution. Because of the long c axis (234 Å) data collection was limited to 2.4 Å resolution. The crystal properties and data collection statistics are summarized in Table 2.

The average density of the orthorhombic crystals, based on three measurements, is 1.23 ± 0.016 g cm^{-3}. Using this density, the calculated molecular weight of protein per asymmetric unit is (M_p) about 568 220 Da. With a calculated molecular weight of 77 435 Da for each monomer of YAO based on the predicted protein sequence (Bruinenberg, Evers, Waterham, Kuipers, Arnberg & Ab, 1989), the calculated number of dimers in the asymmetric unit would be 3.7. The specific volume (V_M) corresponding to three or four dimers in the asymmetric unit is 2.6 or 1.9 Å^3 Da^{-1}; both of these

values are acceptable compared with other proteins of this size (Matthews, 1968), but the former is more likely.

3.2. Molecular replacement

Molecular replacement was applied to obtain initial protein phases for YAO using the ECAO structure as a search probe. The search model was modified by removing side-chain atoms from the model; a main-chain only search model seemed to work best. 11 peptide segments were also omitted from the ECAO search probe. The first omitted segment includes the N-terminus from 5 to 71 in ECAO which is not coded by the YAO gene (Tipping & McPherson, 1995). The remaining ten omitted segments occur in loops in ECAO and are weakly homologous to YAO and most other CAO's.

The initial rotation/translation search using *AMoRe* was limited to a 15.0–5.5 Å resolution shell. The top 50 peaks from the cross-rotation function were used for a translation-function search. After locating the first dimer in a one-body search, the positions of two additional dimers were found relative to the first one using a three-body search. Rigid-body refinement was applied after each translation-function search. The top unique solution after the translation function and rigid-body refinement had a correlation coefficient of 39.1 and R factor 45.3% compared with values of 30.2 and 47.5, respectively, for the next best solution. The orientations of the three dimers in the top solution correspond to the first, third and fifth peaks from the cross-rotation function.

The packing arrangement of the three dimers was obtained by application of the three transformation operations from the top molecular-replacement solution to the original ECAO coordinates, and was analyzed on the graphics display using *O* and by geometric analysis using *X-PLOR*. Fig. 2 is a stereoview of the crystal
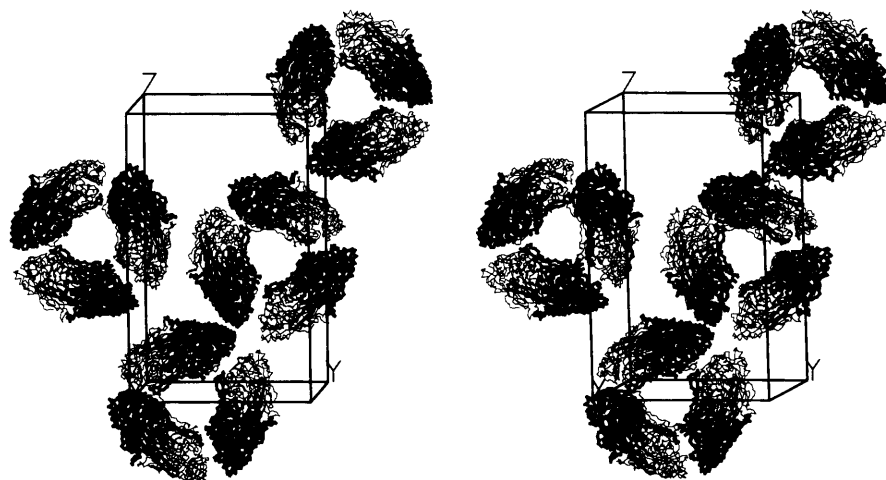

Fig. 2. Stereoview of the molecular packing in the unit cell of form *B* orthorhombic crystals of YAO. Four asymmetric units (12 dimers) are shown. Individual monomers in each dimer are distinguished by line thickness.

packing in the unit cell. Some bad contacts were found in the region from residues 226–240 and this segment was subsequently omitted from the model. This region is poorly conserved and corresponds to a loop in ECAO. Dimers were then translated into one asymmetric unit in order to display the non-crystallographic symmetry (NCS) (Fig. 3). The model consists of a trigonal arrangement which has $D3$ (32) point-group symmetry. There is a non-crystallographic threefold axis parallel to a crystallographic twofold screw axis in the a direction of the unit cell. The local twofold axes of each dimer are separated by 120°. The orientation of each of the dyads in the unit cell is indicated by the angles with respect to the unit-cell edges in the b and c directions (Fig. 3).

The molecular-replacement results are strongly supported by the self-rotation function calculated from the X-ray data for YAO. This function, calculated in spherical polar angles at 3.0 Å resolution, shows strong peaks in the $\kappa = 60$ and 120° sections at $\varphi = 0°$ with magnitude 86% of the crystallographic origin peaks (Fig. 4) and indicates that there is sixfold symmetry in Patterson space. There are also strong peaks in the

$\kappa = 180°$ section at $\varphi = 90$ or $-90°$ and at $\omega = 30$ and 60°. All of these peaks can be explained by the non-crystallographic threefold axis relating dimers in the YAO cell when combined with the crystallographic twofold symmetry of the orthorhombic unit cell.

The secondary non-crystallographic symmetry peaks (64% of peak hight) at $\kappa = 180°$, $\varphi = 90°$, and $\omega = 12.5$, 17.7, 42.5, 47.6, 72.3 and 77.5° (Fig. 5) can be explained by the local twofold symmetries relating YAO monomers (Fig. 3). The local twofold axis in the bc plane, inclined to the b axis by 12.5°, generates all six of these secondary peaks when combined with the threefold NCS and twofold crystallographic symmetry.

Refinement of the initial model was carried out using X-PLOR (version 3.1). With strict NCS (Brünger, 1992), the size of the model was reduced to only one monomer in the asymmetric unit. Rigid-body refinement using X-PLOR was done by separating the monomer into three domains. Molecular dynamics
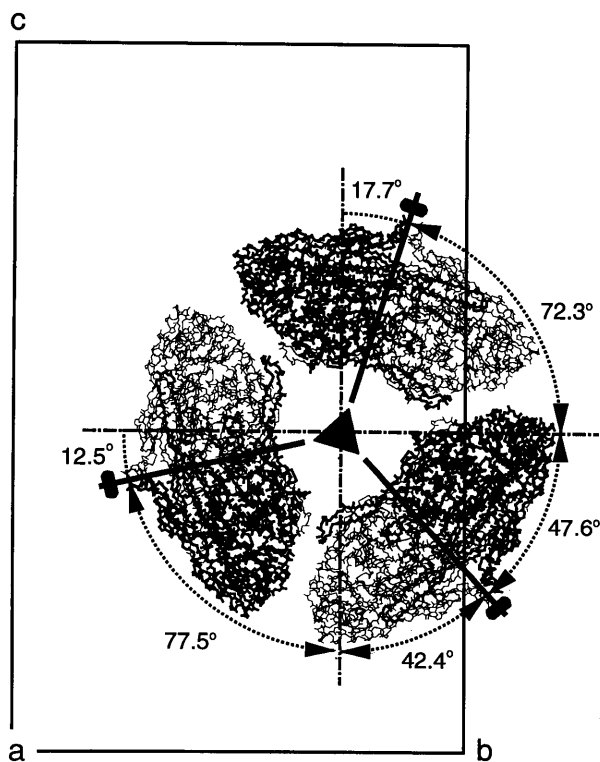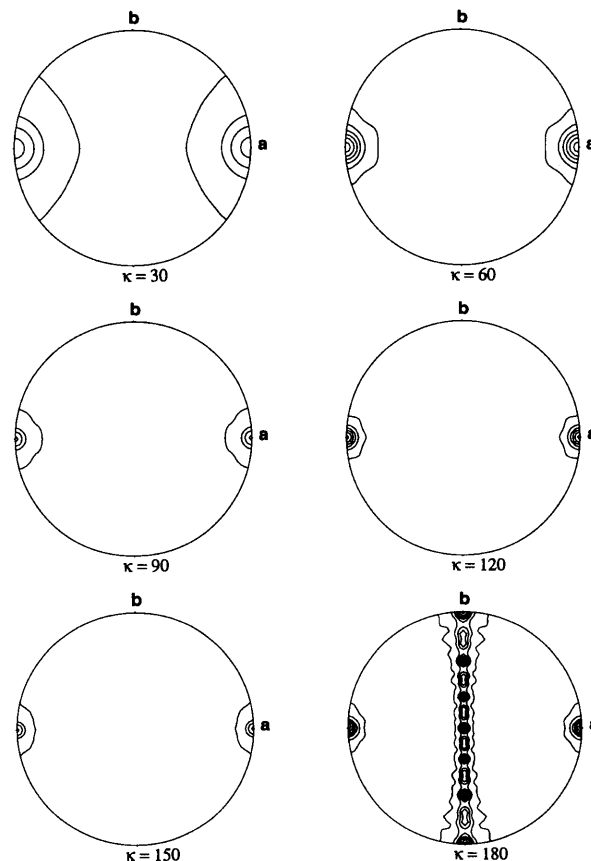

Fig. 3. Schematic drawing of the crystallographic asymmetric unit based on the molecular-replacement solution. The asymmetric unit consists of a trigonal arrangement of dimers and has point-group symmetry $D3$ (32), with the local threefold axis parallel to the crystallographic a axis. The directions of the dyads in each dimer (the monomers are distinguished by thin and thick lines) are indicated with respect to the crystallographic b and c axes.

Fig. 4. Stereographic projection for selected sections in κ (the rotation angle) of the self-rotation function using data between 8.0 and 3.0 Å resolution from the native YAO data set. The Patterson integration radius is 30.0 Å and the stepsize is 5°. The plot is contoured starting at a value of 2σ with a stepsize of 1.5σ. $\omega = 0$ or 180° are at the center, $\omega = 90°$ at the edge; the direction for $\varphi = 0°$ is parallel to a and increases anticlockwise around the periphery.

refinement using the slow-cooling protocol (Brünger, Krukowski & Erickson, 1990) with an initial temperature of 3 000 K and conjugate-gradient minimization was then carried out. The non-conserved side chains of ECAO were replaced with those of YAO based on the sequence alignment, and the conformation of the side chains and main chains were adjusted based on the $(2F_o - F_c)$ electron-density map. Further refinement of the model using 85% of the protein gave a conventional R value of 31.0% and free R of 37% with good geometry.

The refined partial model provided initial phases for solving the potassium mercuric iodide derivative of YAO. Based on the refined molecular-replacement phases, a difference electron-density map using $(F_{HP} - F_P)$ as coefficients, where F_{HP} and F_P are the structure factors for the mercuric derivative and native protein, respectively, showed 12 peaks in the asymmetric unit which segregated into two sites for each monomer, each obeying the NCS. The fact that the binding sites for mercury are close to cysteine side chains in the YAO model provides independent chemical evidence that the molecular replacement model is correct. The ability to locate 12 mercury binding sites in the potassium mercuric iodide derivative of YAO using the molecular-replacement phases provides the opportunity to carry out sixfold averaging and solvent flattening of this single isomorphous derivative of YAO. This procedure should greatly

improve the quality of the map and allow a structural interpretation to be made. The resulting model should be unbiased with respect to the starting model of ECAO used in the molecular-replacement procedure and should lead to rapid convergence to the correct structure. Efforts along these lines are currently in progress.

Fig. 5. Stereographic projection for the section $\kappa = 180°$ of the self-rotation function from the native YAO data set (resolution 8.0–3.0 Å). The Patterson integration radius is 30.0 Å and the stepsize is 5°. The plot is contoured starting at a value of 2.0σ with a stepsize of 1.0σ. The peaks in $\omega = 0$ to 90° are marked with the relative peak heights in parentheses. The direction of $\varphi = 0°$ is parallel to the a cell edge and increases anticlockwise around the periphery.

References

Ameyama, M., Hayashi, U., Matsushita, K., Shinagawa, E. & Adachi, I. (1984). *Agric. Biol. Chem.* **48**, 561–565.

Bachrach, U. (1985). *Structure and Functions of Amine Oxidases*, edited by B. Mondovi, pp. 5–20. Boca Raton: CRC Press.

Blundell, T. L. & Johnson, L. N. (1976). *Protein Crystallography*. New York: Academic Press.

Bruinenberg, P. G., Evers, M., Waterham, H. R., Kuipers, J., Arnberg, A. C. & Ab, G. (1989). *Biochem. Biophys. Acta*, **1008**, 157–167.

Brünger, A. T. (1992). *X-PLOR version 3.1. A system for X-ray crystallography and NMR*. Yale University, CT, USA.

Brünger, A. T., Krukowski, A. & Erickson, J. (1990). *Acta Cryst.* A**46**, 583–593.

Cai, D. & Klinman, J. P. (1994a). *J. Biol. Chem.* **269**, 32039–32042.

Cai, D. & Klinman, J. P. (1994b). *Biochemistry*, **33**, 7647–7653.

Carter, C. W. Jr. & Carter, C. W. (1979). *J. Biol. Chem.* **254**, 12219–12223.

Collaborative Computational Project, Number 4 (1994). *Acta Cryst.* D**50**, 760–763.

Cudney, R., Patel, S., Weisgraber, K., Newhouse, Y. & McPherson, A. (1994). *Acta Cryst.* D**50**, 414–423.

Dooley, D. M., McGuirl, M. A., Brown, D. E., Turowski, P. N., McIntire, W. S. & Knowles, P. F. (1991). *Nature (London)*, **349**, 262–264.

Fontecave, M. & Eklund, H. (1995). *Structure*, **3**, 1127–1129.

Hamilton, G. A. (1968). *Pyridoxal Catalysis: Enzyme and Model Systems*, Vol. 35, edited by E. E. Snell, A. E. Braustein, E. S. Severin & Yu. M. Torchinsky, pp. 375–390. New York: Wiley Interscience.

Hartmann, C. & Dooley, D. M. (1995). *Methods Enzymol.* **258**, 69–90.

Jancarik, J. A. & Kim, S.-H. (1991). *J. Appl. Cryst.* **24**, 409–411.

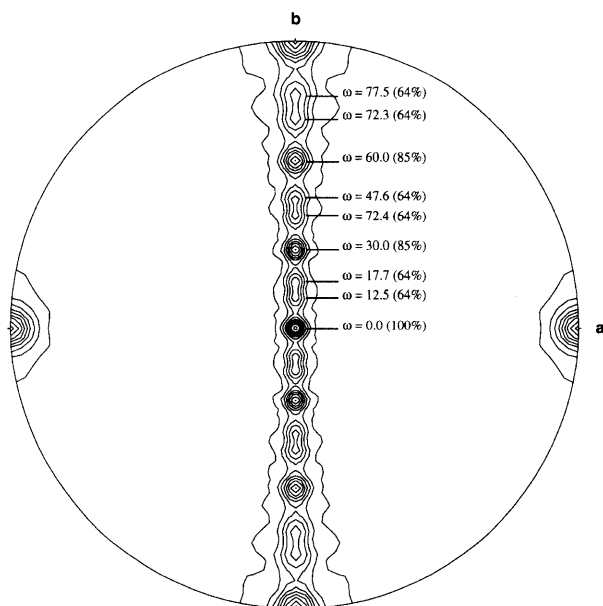Janes, S. M. & Kinman, J. P. (1995). *Methods Enzymol.* **258**, 20–33.

Janes, S. M., Mu, D., Wemmer, D., Smith, A. J., Kaur, S., Maltby, D., Burlingame, A. L. & Klinman, J. P. (1990). *Science*, **248**, 981–986.

Janes, S. M., Palcic, M. M., Scanman, C. H., Smith, A. J., Brown, D. E., Dooley, D. M., Mure, M. & Klinman, J. P. (1992). *Biochemistry*, **31**, 12147–12154.

Janne, J., Posa, A. & Raina, A. (1978). *Biochem. Biophys Acta*, **473**, 241–293.

Jones, T. A. (1978). *J. Appl. Cryst.* **11**, 268–272.

Klinman, J. P. & Mu, D. (1994). *Annu. Rev. Biochem.* **63**, 299–344.

Knowles, P. F. & Dooley, D. M. (1994). *Metal Ions in Biological Systems*, edited by H. Sigel & A. Sigel, pp. 361–403. New York: Marcel Dekker.

Kumar, V., Dooley, D. M., Freeman, H. C., Guss, J. M., Harvey, I., McGuirl, M. A., Wilce, M. C. J. & Zubak, V. M. (1996). *Structure*, **4**, 943–955.

Lobenstein-Verbeek, C. L., Jongejan, J. A., Frank, J. & Durine, J. A. (1984). *FEBS Lett.* **170**, 305–309.

Low, B. W. & Richards, F. M. (1952). *J. Am. Chem. Soc.* **74**, 1660–1666.

McCann, P. P., Pegg, A. E. & Sjoerdsma, A. (1987). *Inhibition of Polyamine Metabolism: Biological Significance and Basis for New Therapies.* Orlando: Academic Press.

McIntire, W. S. & Hartmann, C. (1992). *Principles and Application of Quinoproteins*, edited by V. L. Davidson, pp. 97–171. New York: Marcel Dekker.

Mathews, F. S. (1995). *Methods Enzymol.* **258**, 191–216.

Matsuzaki, R., Fukui, T., Sato, H., Ozaki, Y. & Tanizawa, K. (1994). *FEBS Lett.* **351**, 360–364.

Matthews, B. W. (1968). *J. Mol. Biol.* **33**, 491–497.

Matthews, B. W. (1974). *J. Mol. Biol.* **82**, 513–526.

Mu, D., Janes, S. M., Smith, A. J., Brown, D. E., Dooley, D. M. & Klinman, J. P. (1992). *J. Biol. Chem.* **267**, 7979–7982.

Navaza, J. (1994). *Acta Cryst.* A**50**, 157–163.

Otwinowski, Z. (1993). *DENZO. An Oscillation Data Processing Suite for Macromolecular Crystallography.* Yale University, New Haven, CT, USA.

Parsons, M. R., Convery, M. A., Wilmot, C. M., Yadav, K. D. S., Blakeley, V., Corner, A. S., Philips, S. E. V., McPherson, M. J. & Knowles, P. F. (1995). *Structure*, **3**, 1171–1184.

Tipping, A. J. & McPherson, M. J. (1995). *J. Biol. Chem.* **270**, 16939–16946.

Zwart, K., Veenhuis, M., van Dijken, J. P. & Harder, W. (1980). *Arch. Microbiol.* **126**, 117–126.